

FTUAM-93/01
CRN/PT 93-39
nucl-th/9307001
October, 1993

A Full pf Shell Model Study of $A = 48$ Nuclei

E. Caurier, A. P. Zuker

Groupe de Physique Théorique
CRN IN2P3-CNRS/Université Louis Pasteur BP20
F-67037 Strasbourg-Cedex, France

A. Poves and G. Martínez-Pinedo

Departamento de Física Teórica C-XI
Universidad Autónoma de Madrid
E-28049 Madrid, Spain.

Abstract

Exact diagonalizations with a minimally modified realistic force lead to detailed agreement with measured level schemes and electromagnetic transitions in ^{48}Ca , ^{48}Sc , ^{48}Ti , ^{48}V , ^{48}Cr and ^{48}Mn . Gamow-Teller strength functions are systematically calculated and reproduce the data to within the standard quenching factor. Their fine structure indicates that fragmentation makes much strength unobservable. As a by-product, the calculations suggest a microscopic description of the onset of rotational motion. The spectroscopic quality of the results provides strong arguments in favour of the general validity of monopole corrected realistic forces, which is discussed.

1 Introduction

Exact diagonalizations in a full major oscillator shell are the privileged tools for spectroscopic studies up to $A \approx 60$. The total number of states $—2^d$ with $d = 12, 24$ and 40 in the p , sd , and pf shells respectively— increases so fast that three generations of computers and computer codes have been necessary to move from $n = 4$ to $n = 8$ in the pf shell i.e. from four to eight valence particles, which is our subject.

A peculiarity of the pf shell is that a minimally modified realistic interaction has been waiting for some 15 years to be tested in exact calculations *with sufficiently large number of particles*, and $n = 8$ happens to be the smallest for which success was practically guaranteed. In the test, spectra and electromagnetic transitions will be given due place but the emphasis will go to processes governed by spin operators: beta decays, (p, n) and (n, p) reactions. They are interesting —perhaps fascinating is a better word— on two counts. They demand a firm understanding of not simply a few, but very many levels of given J and they raise the problem of quenching of the Gamow-Teller strength.

As by-products, the calculations provide clues on rotational motion and some helpful indications about possible truncations of the spaces. The paper is arranged as follows.

Section 2 contains the definition of the operators. Some preliminary comments on the interaction are made.

In each of the following six sections, next to the name of the nucleus to which it is devoted, the title contains a comment directing attention to a point of interest. The one for ^{48}Ca is somewhat anomalous.

In section 9, the evidence collected on GT strength is analyzed. Our calculations reproduce the data once the standard quenching factor, $(0.77)^2$, is adopted. The fine structure of the strength function indicates that fragmentation makes impossible the observation of many peaks. Several experimental checks are suggested. Minor discrepancies with the data are attributed to small uncertainties in the $\sigma \cdot \sigma$ and $\sigma\tau \cdot \sigma\tau$ contributions to the force.

In section 10 we examine the following question:

Why, in the sd shell, phenomenologically fitted matrix elements have been so far necessary to yield results of a quality comparable with the ones we obtain here with a minimally modified realistic interaction? The short answer is that *monopole* corrected realistic forces are valid in general, but the fact is easier to detect in the pf shell.

Section 11 contains a brief note on binding energies. In section 12 we conclude.

The rest of the introduction is devoted to a point of notation, a review of previous work (perhaps not exhaustive enough, for which we apologize) and a word on the diagonalizations.

Notations. Throughout the paper f stands for $f_{7/2}$ (except of course when we speak of the pf shell) and r , generically, for any or all of the other subshells ($p_{1/2}$ $p_{3/2}$ $f_{5/2}$). Spaces of the type

$$f^{n-n_0}r^{n_0} + f^{n-n_0-1}r^{n_0+1} + \dots + f^{n-n_0-t}r^{n_0+t} \quad (1)$$

represent possible truncations: n_0 is different from zero if more than 8 neutrons are present and when $t = n - n_0$ we have the full space $(pf)^n$ for $A = 40 + n$.

Bibliographical note. The characteristic that makes the pf shell unique in the periodic table is that at $t = 0$ we already obtain a very reasonable model space, as demonstrated in the f^n case (i.e. $n_0 = 0$) by Ginocchio and French [1] and Mc Cullen, Bayman and Zamick [2] (MBZ in what follows). The $n_0 \neq 0$ nuclei are technically more demanding but the $t = 0$ approximation is again excellent (Horie and Ogawa [3]).

The first systematic study of the truncation hierarchy was undertaken by Pasquini and Zuker [4, 5] who found that $t = 1$ has beneficial effects, $t = 2$ may be dangerous and even nonsensical, while $t = 3$ restored sense in the only non trivial case tractable at the time (^{56}Ni). This seems to be generally a fair approximation, and the topic will be discussed as we proceed.

Much work on $n_0 \neq 0$ nuclei with $t = 1$ and 2 spaces was done by the groups in Utrecht (Glaudemans, Van Hees and Mooy [6, 7, 8] and Tokyo (Horie, Muto, Yokohama [9, 10, 11]).

For the Ca isotopes high t and even full space diagonalizations have been possible (Halbert, Wildenthal and Mc Grory [12, 13]).

Exact calculations for $n \leq 4$ are due to Mc Grory [14], and some $n = 5$ nuclei were studied by Cole [15] and by Richter, Van der Merwe, Julies and Brown in a paper in which two sets of interaction matrix elements are constructed [16].

For $n = 6, 7$ and 8 the only exact results reported so far are those of the authors on the magnetic properties of the Ti isotopes [17], and the double β decay calculations of ^{48}Ca by Ogawa and Horie [18], the authors [19] and Engel, Haxton and Vogel [20]. The MBZ model has been reviewed in an appendix to Pasquini's thesis [4] and by Kutschera, Brown and Ogawa [21]. Its success suggested the implementation of a perturbative treatment in the full pf shell by Poves and Zuker [22, 23].

All the experimental results for which no explicit credit is given come from the recent compilation of Burrows for $A = 48$ [24].

	^{48}Ca	^{48}Sc	^{48}Ti	^{48}V	^{48}Cr
m-scheme	12 022	139 046	634 744	1 489 168	1 963 461
J T	4 4	4 3	4 2	5 1	4 0
	1 755	17 166	63 757	106 225	58 219

Table 1: m-scheme and maximal JT dimensions in the full pf shell

The diagonalizations are performed in the m -scheme using a fast implementation of the Lanczos algorithm through the code ANTOINE [25]. Some details may be found in ref. [26]. The strength functions are obtained through Whitehead's prescription [27], explained and illustrated in refs. [17, 19] (and section 9). The m -scheme and maximal JT dimensions of the nuclei analyzed are given in table 1. To the best of our knowledge they are the largest attained so far.

2 The Interaction and other Operators

The most interesting result of refs. [4, 5] was that the spectroscopic catastrophes generated by the Kuo-Brown interaction [28] in some nuclei, could be cured by the simple modification (KB' in [4, 5]).

$$V_{fr}^T(\text{KB1}) = V_{fr}^T(\text{KB}) - (-)^T 300 \text{ keV} \quad (2)$$

where V_{fr}^T are the centroids, defined for any two shells by

$$V_{ij}^T = \frac{\sum_J (2J+1) W_{ijij}^{JT}}{\sum_J (2J+1)}, \quad (3)$$

where the sums run over Pauli allowed values if $i = j$, and W_{ijij}^{JT} are two body matrix elements. For $i, j \equiv r$, no defects can be detected until much higher in the pf region. On the contrary, the calculations are quite sensitive to changes in W_{ffff}^{JT} but the only ones that are compulsory affect the centroids and it is the binding energies that are sensitive to them:

$$\begin{aligned} V_{ff}^0(\text{KB1}) &= V_{ff}^0(\text{KB}) - 350 \text{ keV} \\ V_{ff}^1(\text{KB1}) &= V_{ff}^1(\text{KB}) - 110 \text{ keV}. \end{aligned} \quad (4)$$

The interaction we use in the paper, KB3, was defined in ref. [23] as

$$\begin{aligned} W_{ffff}^{J0}(\text{KB3}) &= W_{ffff}^{J0}(\text{KB1}) - 300 \text{ keV for } J = 1, 3 \\ W_{ffff}^{21}(\text{KB3}) &= W_{ffff}^{21}(\text{KB1}) - 200 \text{ keV}. \end{aligned} \quad (5)$$

while the other matrix elements are modified so as to keep the centroids (4).

It should be understood that the minimal interaction is KB1 in that the bad behaviour of the centroids reflects the bad saturation properties of the realistic potentials: if we do not accept corrections to the centroids we have no realistic interaction. Compared with the statements in eqs. (2) and (4), eq. (5) is very small talk that could just as well be ignored. However, to indulge in it is of some interest, as will become apparent in section 10.

In what follows, and unless specified otherwise, we use

- harmonic oscillator wave functions with $b = 1.93 \text{ fm}$
- bare electromagnetic factors in $M1$ transitions; effective charges of 1.5 e for protons and 0.5 e for neutrons in the electric quadrupole transitions and moments.
- Gamow-Teller (GT) strength defined through

$$B(GT) = \kappa^2 \langle \sigma \tau \rangle^2, \quad \langle \sigma \tau \rangle = \frac{\langle f | \sum_k \sigma^k t_{\pm}^k | i \rangle}{\sqrt{2J_i + 1}}, \quad (6)$$

where the matrix element is reduced with respect to the spin operator only (Racah convention [29]) and κ is the axial to vector ratio for GT decays.

$$\kappa = (g_A/g_V)_{\text{eff}} = 0.77(g_A/g_V)_{\text{bare}} = 0.963(7). \quad (7)$$

- for the Fermi decays we have

$$B(F) = \langle \tau \rangle^2, \quad \langle \tau \rangle = \frac{\langle f || \sum_k t_{\pm}^k || i \rangle}{\sqrt{2J_i + 1}} \quad (8)$$

- half-lives, t , are found through

$$(f_A + f^\epsilon)t = \frac{6170 \pm 4}{(f_V/f_A)B(F) + B(GT)} \quad (9)$$

We follow ref. [30] in the calculation of the f_A and f_V integrals and ref. [31] for f^ϵ . The experimental energies are used.

3 ⁴⁸Ca ERRATUM

In fig. 1 we compare calculated and experimental levels. Except for the lowest 2^+ state the agreement is good and the first excited 0^+ is certainly an intruder.

The calculated $M1$ strength is found in a triplet (not shown) at excitation energies of 9.82, 10.06 and 10.23 MeV with $B(M1)$ values of 0.39, 6.17 and $1.81 \mu_N^2$, respectively, which nearly exhaust the sum rule of $8.96 \mu_N^2$. The total observed strength between 7.5 and 12.5 MeV is $5.2 \pm 0.5 \mu_N^2$. It is dominated by the majestic peak at 10.2 MeV ($3.9 \mu_N^2$) and otherwise fragmented among some twenty states; below 11.7 MeV there are 14 peaks where the calculation only produce 8. The observed to calculated ratio $5.2/8.96 = (0.76)^2$, is very much the standard value for spin-like operators.

The $E2$ rates

$$\begin{aligned} B(E2, 4^+ \rightarrow 2^+) &= 2.65 \text{ e}^2 \text{ fm}^4 \\ B(E2, 2^+ \rightarrow 0^+) &= 10.2 \text{ e}^2 \text{ fm}^4 \end{aligned} \quad (10)$$

agree reasonably with the experimental values

$$\begin{aligned} B(E2, 4^+ \rightarrow 2^+)_{\text{exp}} &= 1.89 \text{ e}^2 \text{ fm}^4 \\ B(E2, 2^+ \rightarrow 0^+)_{\text{exp}} &= 17.2 \text{ e}^2 \text{ fm}^4 \end{aligned} \quad (11)$$

but definitely suggest that something is missing in a strict $0\hbar\omega$ calculation.

In ref. [19] we studied 2ν double β decay of ⁴⁸Ca and calculated the strength functions for the associated processes ⁴⁸Ca(p, n)⁴⁸Sc and ⁴⁸Ti(n, p)⁴⁸Sc, and for the latter we have to offer the following:

ERRATUM. The total ⁴⁸Ti(n, p) strength in ref. [19] misses a factor 3/2. Hence the ⁴⁸Ca 2ν double β decay half-life has to be multiplied by a factor 2/3 to yield $T_{1/2} = 3.7 \cdot 10^{19}$ yr.

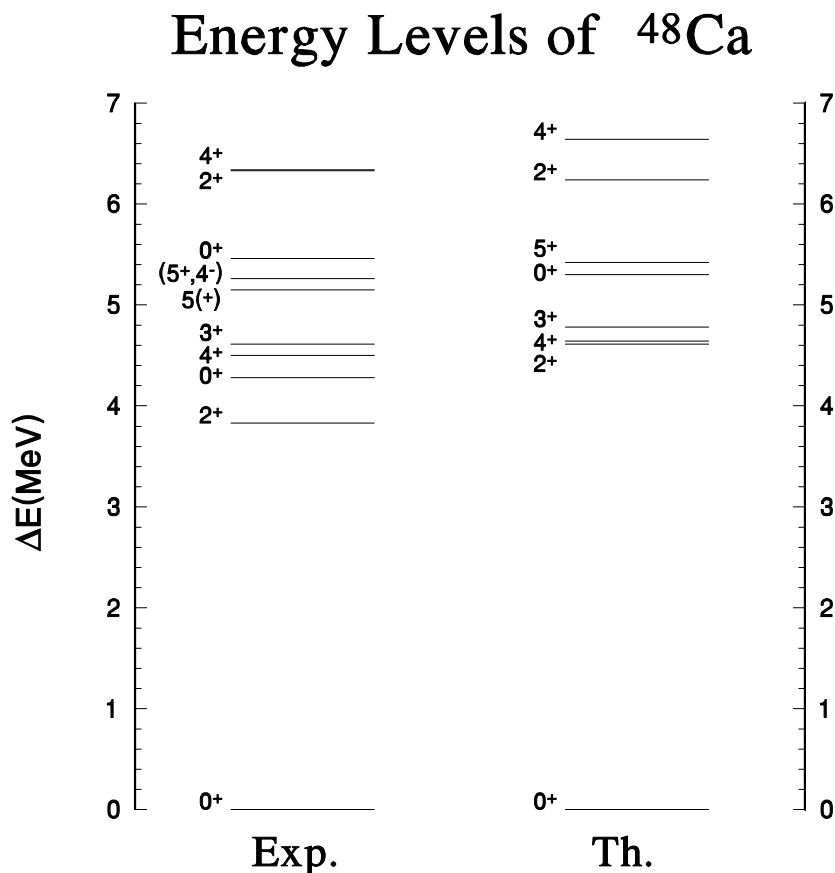


Figure 1: Experimental and theoretical energy levels of ^{48}Ca

4 ^{48}Sc The famous seven

The $J = 1 - 7$, $T = 3$, multiplet of “ f^8 ” states in ^{48}Sc can be related to “ f^2 ” states in ^{42}Sc through a Racah coefficient (the Pandya-Talmi transformation). The operation is successful enough to have become a textbook example. There are some discrepancies that are removed by a $t=1$ truncation, hailed in ref. [5] as a triumph of the realistic forces. These levels change very little in going from $t=1$ to perturbative [22, 23] and then to the exact results, but they are quite sensitive to changes in the W_{ffff} matrix elements. In all the other nuclei the situation is reversed and figure 2 provides the *only* example of an exact calculation that does not bring an improvement over the approximate ones. Note however that the agreement with data is definitely good, and extends to three levels at around 2 MeV that do not belong to the multiplet. Below 2.5 MeV there are a couple of 2^+ states with no calculated counterparts, i.e. intruders. A more complete view of the density of intruders comes from table 2, where we have listed the 9 calculated 1^+ levels below 6 MeV against 13 experimental candidates [32]. Immediately above 6 MeV, diagonalizations yield level spacings of 100 keV. The number of intruders will also grow fast and one to one identifications become meaningless because the number of levels that can

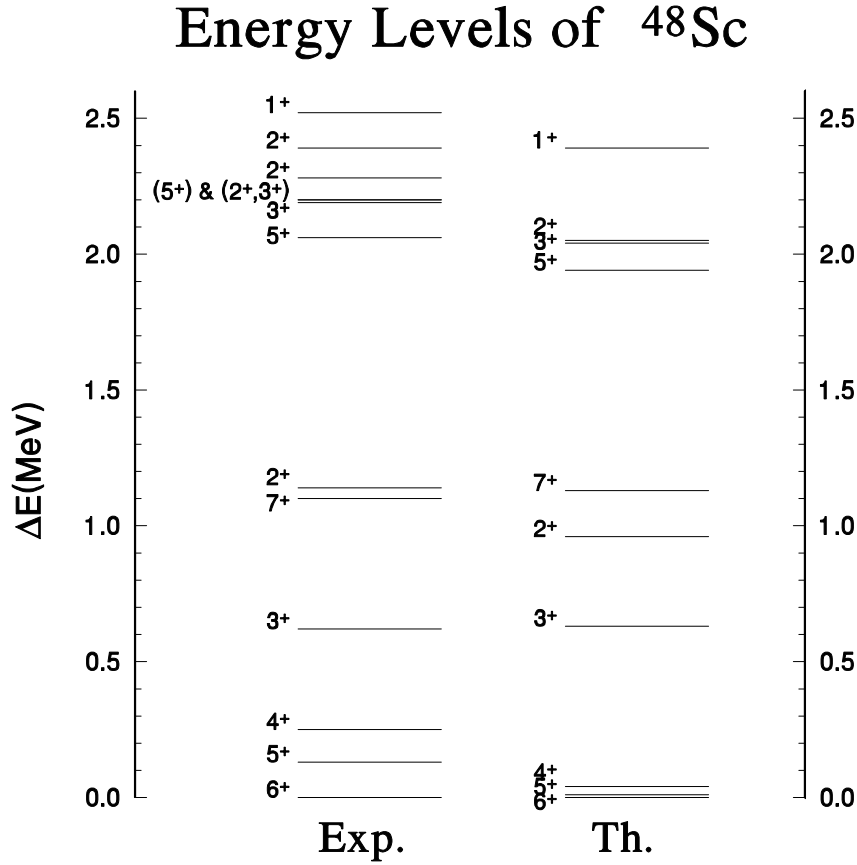


Figure 2: Experimental and theoretical energy levels of ^{48}Sc

be observed becomes small fraction of those present. Note that even some of the calculated states in table 2 may have escaped detection (e.g. the one at 5.23 MeV).

Exp	2.52	2.98	3.06	3.16	3.26	3.71	4.00	4.18	4.32	4.68	4.78	5.45	5.74
Th	2.39	2.91			3.46		3.95		4.49	4.67	5.23	5.49	5.79

Table 2: 1^+ states in ^{48}Sc . Energies in MeV.

^{48}Sc decays to ^{48}Ti *via* the doublet of 6^+ states at 3.33 and 3.51 MeV. The measured half-life, $\log ft$ values and branching ratios are

$$\begin{aligned}
 T_{1/2} &= 43.7 \text{ h} \\
 \log ft(6_1^+) &= 5.53 \quad \% \beta = 90.7\% \\
 \log ft(6_2^+) &= 6.01 \quad \% \beta = 9.3\%
 \end{aligned}
 \tag{12}$$

while the calculated ones read

$$\begin{aligned}
T_{1/2} &= 29.14 \text{ h} \\
\log ft(6_1^+) &= 5.34 \quad \% \beta = 96\% \\
\log ft(6_2^+) &= 6.09 \quad \% \beta = 4\%
\end{aligned}
\tag{13}$$

We have here a first example of the extreme sensitivity of the half-lives to effects that are bound to produce very minor changes in other properties that are satisfactorily described, such as those of the 6^+ doublet (see next section).

5 ^{48}Ti Intrinsic states

Experimentally this is the richest of the $A = 48$ nuclei. The lines in fig. 3 connect theoretical levels (to the right) with observed ones (to the left). The agreement, which would be perfect if all lines were horizontal, is nevertheless quite good: the rms deviation for the 33 excited states is of 110 keV. Dots correspond to the first intruders detected for a given J value.

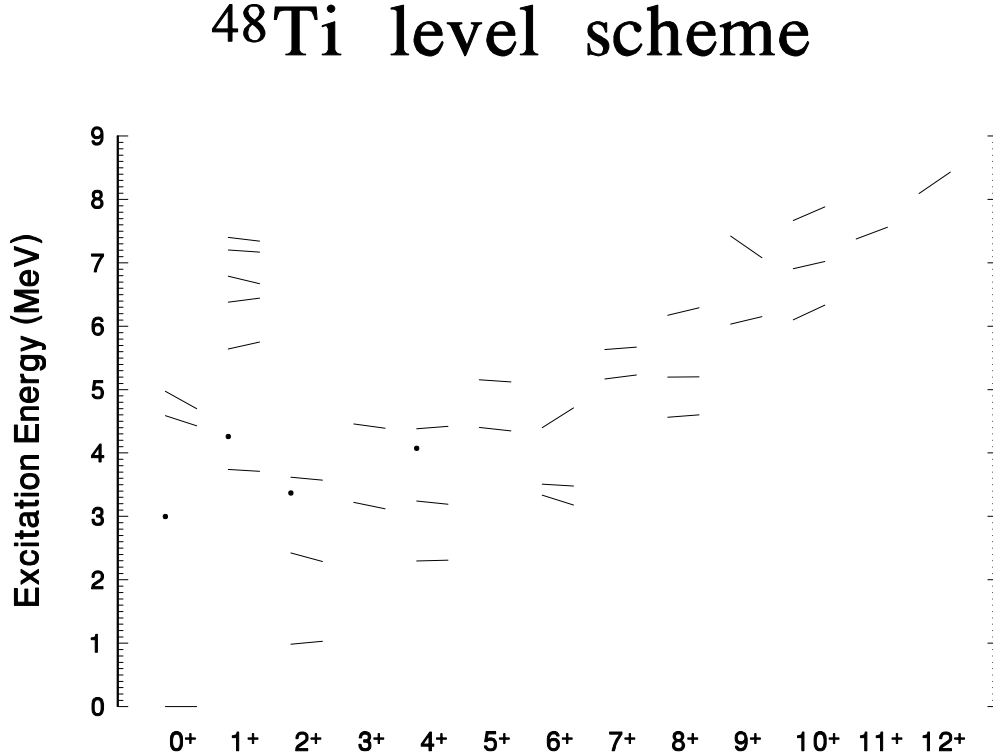


Figure 3: Experimental and theoretical energy level of ^{48}Ti . The left side of the lines corresponds to the experimental value, the right side corresponds to the theoretical one. The isolated points are intruder states not included in our valence space

Tables 3 and 4 contain the information on $E2$ and $M1$ transitions, to which we may add the magnetic moment of the first 2^+ state, calculated to be $\mu(2^+) = 0.43 \mu_N$, lowish with respect of the measured $\mu(2^+) = 0.86 (38) \mu_N$ and $\mu(2^+) = 1.12 (22) \mu_N$ [33].

$J_n^\pi(i)$	$J_m^\pi(f)$	EXP	$(fp)^8$	$f^8(^{42}\text{Sc})$
2_1^+	0_1^+	142 ± 6	92.1	52.9
4_1^+	2_1^+	111 ± 20	136.6	65.8
2_2^+	2_1^+	104 ± 104	36.0	45.2
2_2^+	0_1^+	13 ± 2	20.3	6.6
2_3^+	0_1^+	22 ± 6	4.3	0.2
6_1^+	4_1^+	52 ± 5	54.8	39.3
6_2^+	4_1^+	56 ± 25	55.5	0.7
6_3^+	4_1^+	75 ± 30	34.1	29.8
8_1^+	6_2^+	<14.5	20.2	4.6
8_1^+	6_1^+	<51.8	63.4	41.4
8_2^+	6_2^+	74 ± 40	46.6	32.4
8_2^+	6_1^+	9_{-4}^{+9}	10.7	2.2
10_1^+	8_1^+	<46.6	46.7	32.9
9_2^+	9_1^+	<39.4	11.8	11.7

Table 3: ^{48}Ti $E2$ transitions, $B(E2)$ in $\text{e}^2 \text{fm}^4$. $f^8(^{42}\text{Sc})$ is a $t=0$ calculation with W_{ffff} matrix elements taken from the spectrum of ^{42}Sc .

There are very few discrepancies between the exact calculations $(fp)^8$, and the data and they are hardly significant. Remarkably enough this could also be said of the f^8 calculations, for the $M1$ transitions and to some extent for the $B(E2)$ with the spectacular exception in $B(E2, 6_{1,2}^+ \rightarrow 4_1^+)$. The exact results build enough quadrupole coherence with standard effective charges but the truly important difference with the $t=0$ calculations shows in table 5, where we have collected the intrinsic quadrupole moment Q_0 , extracted from the spectroscopic ones through

$$Q_0 = \frac{(J+1)(2J+3)}{3K^2 - J(J+1)} Q_{\text{spec}}(J), \quad (14)$$

setting $K = 0$. For the exact calculations, Q_0 is also extracted through the rotational model prescription

$$B(E2, J \rightarrow J-2) = \frac{5}{16\pi} e^2 |\langle JK20 | J-2, K \rangle|^2 Q_0^2. \quad (15)$$

$J_n^\pi(\text{i})$	$J_m^\pi(\text{f})$	EXP	$(fp)^8$	$f^8(^{42}\text{Sc})$
0_1^+	1_1^+	0.50 ± 0.08	0.54	0.73
0_1^+	1_2^+	0.50 ± 0.08	0.41	
0_1^+	1_5^+	0.80 ± 0.06	0.42	
2_2^+	2_1^+	0.5 ± 0.1	0.55	1.63
3_1^+	2_1^+	<0.01	0.55	1.63
3_1^+	4_1^+	<0.06	0.39	0.82
4_2^+	4_1^+	1.0 ± 0.2	1.78	3.45
2_3^+	2_1^+	0.05 ± 0.01	0.39	0.49
6_2^+	6_1^+	6.7 ± 3.3	2.32	8.96
6_3^+	6_1^+	0.9 ± 0.4	0.06	0.00
5_1^+	6_1^+	>0.36	0.41	1.00
5_2^+	6_2^+	>0.9	0.27	0.68
7_1^+	6_2^+	$0.09^{+0.09}_{-0.04}$	0.15	0.30
7_1^+	6_1^+	$0.14^{+0.14}_{-0.06}$	0.33	0.00
8_2^+	8_1^+	1.61 ± 0.70	1.59	3.38
7_2^+	8_1^+	$0.5^{+0.8}_{-0.2}$	0.82	0.00
7_2^+	6_1^+	$0.07^{+0.10}_{-0.03}$	0.12	0.57
9_1^+	8_2^+	>0.95	0.82	0.00
9_1^+	8_1^+	>0.36	0.57	1.55
8_3^+	7_1^+	$0.3^{+1.3}_{-0.1}$	0.54	1.09
8_3^+	8_1^+	$0.2^{+0.5}_{-0.1}$	0.25	0.00
10_2^+	9_1^+	$0.6^{+1.0}_{-0.3}$	3.60	7.08
11_1^+	10_2^+	>0.36	2.58	5.37
11_1^+	10_1^+	>0.36	0.81	0.00
12_1^+	11_1^+	0.5 ± 0.2	2.32	3.46

Table 4: ^{48}Ti $M1$ transitions, $B(M1)$ in μ_n^2 . See also caption to table 3.

$J_n^\pi(i)$	$(fp)_s^8$	$f^8(^{42}\text{Sc})$	$(f_{7/2}p_{3/2})^8$	$(fp)_t^8$
2_1^+	50.4	-12.25	39.17	68
4_1^+	32.18	-11.83	18.47	69
6_1^+	-44.25	13	13.99	
6_2^+	42	4	-25.18	42
8_1^+	32.54	1.67	31.52	44
10_1^+	46.69	13.34	30.29	37
12_1^+	35.78	28.58	31.64	
$Q_0(2^+)_{\text{exp}} = 62 \pm 3$				

Table 5: ^{48}Ti intrinsic quadrupole moments of the Yrast states in e fm². $(fp)_s^8$ means Q_0 extracted from eq. (14). $(fp)_t^8$ means Q_0 extracted from eq. (15).

The wrong sign for the quadrupole moment is a characteristic of the $t = 0$ calculations. The exact results check well with the known experimental value for the 2^+ but they do much more: the curious mixture of signs and sizes coming out of f^8 , becomes a fairly large and constant number for $(fp)^8$.

Although we cannot speak of rotational motion—which demands a truly constant Q_0 and a $J(J+1)$ spectrum—we *are certainly in the presence of a well defined prolate intrinsic structure*.

This build-up of quadrupole coherence is almost entirely due to mixing with the $p_{3/2}$ orbit, as seen from the results for the $(f_{7/2}p_{3/2})^8$ space.

The strength function for $^{48}\text{Ti}(n,p)^{48}\text{Sc}$ can be found in ref. [19] (remember the erratum though...) and ref. [17] contains a study of the (p,p') and (e,e') processes and an analysis of the orbital, spin and $M1$ strengths. The missing piece of information, $^{48}\text{Ti}(p,n)^{48}\text{V}$, is found in figs. 4 and 5, for $t = 1$ and exact calculations. They show similarity in gross structure: some low energy peaks, a resonance-like middle region and $T = 2$ satellite strength higher up. In details they differ mainly in the position of the resonance, shifted down by some 2 MeV in the exact case. The total strength for the full space $S^- = 13.263 \kappa^2$, combined with $S^+ = 1.263 \kappa^2$ obtained for $^{48}\text{Ti}(n,p)^{48}\text{Sc}$, satisfies the sum rule for the GT operator

$$\sum B(GT^-) - \sum B(GT^+) = S^- - S^+ = 3(N - Z) \kappa^2 \quad (16)$$

The mirror β^+ decay of ^{48}Fe to ^{48}Mn has $Q_\beta = 11.1$ MeV, which covers a large fraction of the strength in fig. 5. Experimentally, a comparison of the β^+ and (p,n) processes seems possible. It would certainly be welcome.

$^{48}\text{Ti} \text{ (p,n) } ^{48}\text{V}$

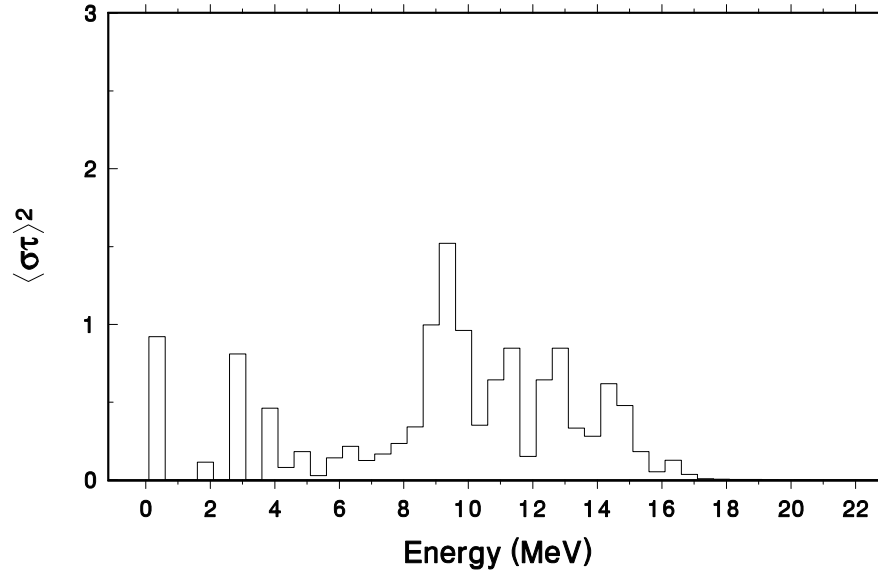


Figure 4: $^{48}\text{Ti} \rightarrow ^{48}\text{V}$ strength function. $t = 1$ calculation

$^{48}\text{Ti} \text{ (p,n) } ^{48}\text{V}$

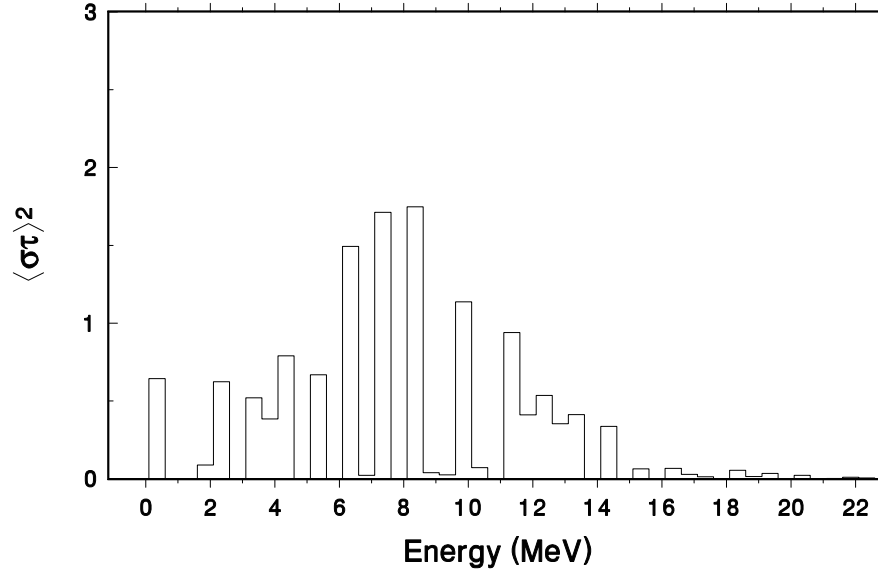


Figure 5: $^{48}\text{Ti} \rightarrow ^{48}\text{V}$ strength function. Full fp-shell calculation

6 ^{48}V The interaction

In fig. 6 we have plotted separately all levels with $J \leq 7$ below 2.5 MeV and the high spin ones. To the repetitive claim that the agreement is excellent we may add a mitigating (i.e. possibly interesting) remark: it is next to impossible to observe the calculated 10^+ and 12^+ states because of the screening provided by their close 11^+ and 13^+ neighbours.

Energy Levels of ^{48}V

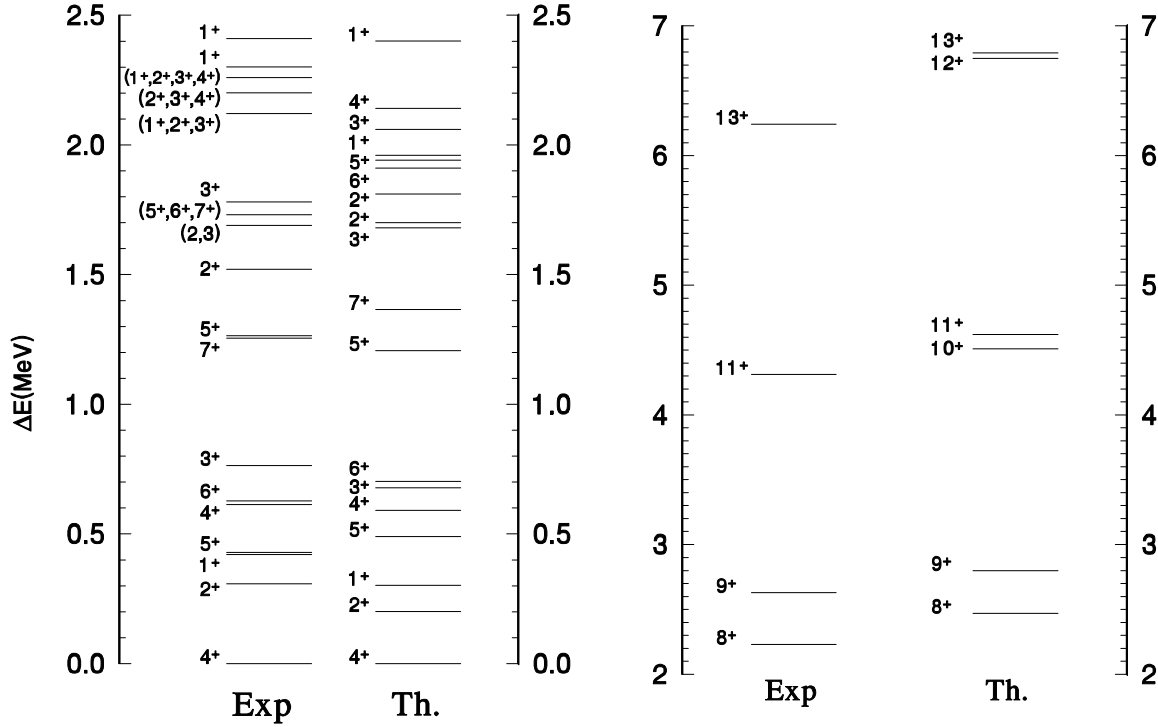


Figure 6: Experimental and theoretical energy levels of ^{48}V

The $M1$ and $E2$ transitions in table 6 show again excellent agreement. For the ground state, $\mu(4^+) = 1.90 \mu_N$ against a measured $\mu(4^+) = 2.01 (1) \mu_N$, while $\mu(2^+) = 0.51 \mu_N$ against two measures $\mu(2^+) = 0.28 (10) \mu_N$ and $0.444 (16) \mu_N$ [33].

The Gamow-Teller β^+ decay to ^{48}Ti can reach $J = 3, 4$ and 5 daughter levels and three of them are fed as shown in table 7. The resulting half life $T_{1/2} = 8.85 \text{ d}$ is almost half the observed one, $T_{1/2} = 15.97 \text{ d}$. The fraction of the total strength responsible for the decay is very small (0.4%). Therefore, the discrepancy in the half-lives could be cured by reducing by half the height of the lowest two bumps in figure 7, which is hardly a change in the overall picture.

$J_n^\pi(\text{i})$	$J_m^\pi(\text{f})$	$B(E2)_{\text{exp}}$	$B(E2)_{\text{th}}$
2_1^+	4_1^+	28.59(17)	48.1
5_1^+	4_1^+	104(42)	209.0
4_2^+	4_1^+	63(25)	28.9
4_2^+	5_1^+	<41	32.0
6_1^+	5_1^+	186(73)	191.0
6_1^+	4_1^+	46(6)	52.0
5_2^+	4_2^+	>176(124)	41.0
2_2^+	2_1^+	>1.3(19)	10.7
$J_n^\pi(\text{i})$	$J_m^\pi(\text{f})$	$B(M1)_{\text{exp}}$	$B(M1)_{\text{th}}$
1_1^+	2_1^+	>0.027	3.12
5_1^+	4_1^+	0.081(14)	0.188
4_2^+	5_1^+	0.045(9)	0.032
4_2^+	4_1^+	0.0084(9)	0.0079
6_1^+	5_1^+	0.027(5)	0.027

Table 6: ^{48}V electromagnetic transitions, $B(E2)$ in $\text{e}^2 \text{fm}^4$ and $B(M1)$ in μ_N^2

J_f	$B(GT)_{\text{th}}$	$B(GT)_{\text{exp}}$
4_1^+	$7.9 \cdot 10^{-3}$	$4.1 \cdot 10^{-3}$
3_1^+	$0.5 \cdot 10^{-3}$	$1.7 \cdot 10^{-3}$
4_2^+	$2.2 \cdot 10^{-3}$	$4.1 \cdot 10^{-3}$

Table 7: $^{48}\text{V} (4^+) \rightarrow ^{48}\text{Ti} (J_f)$ beta decay

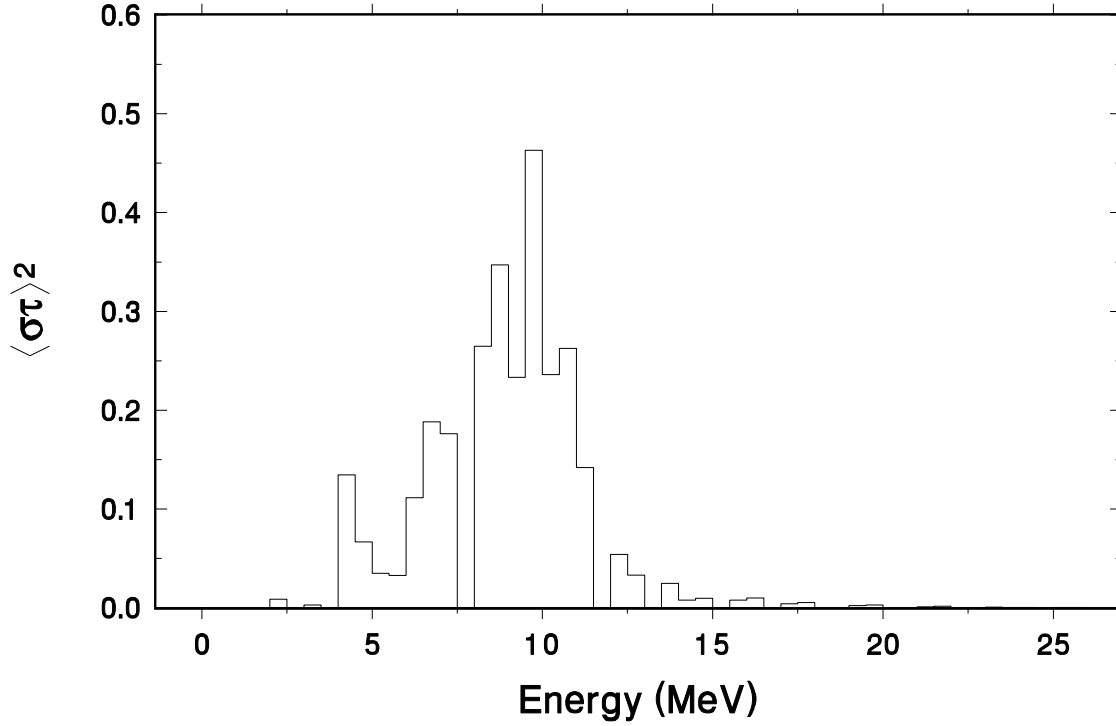
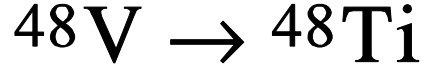


Figure 7: Strength function for the ^{48}V beta decay. Full pf shell calculation

Odd-odd nuclei provide a good test for the interactions and ^{48}V offers a good example of a general trend: perturbative calculations [23] are quite good but the exact results come definitely closer to the data. This systematic improvement clearly indicates that the interaction is excellent. The one exception to the trend comes in ^{48}Sc , and is related to the choice of the KB3 (rather than KB1) interaction. As far as $A = 48$ nuclei are concerned this is an almost irrelevant problem, but there is a conceptual point that will be made clear in section 10.

7 ^{48}Cr Rotational motion

Some levels in ^{48}Cr are populated in the decay of ^{48}Mn and will be discussed in the next section. Beyond that, little is known of the spectrum, except the Yrast line and before we come to it, we go through fig. 8 for the strength function. Only the first 1^+ state is seen through the Q_β window. The calculated half-life is $T_{1/2} = 21.8$ h and the observed one $T_{1/2} = 21.56(3)$ h.

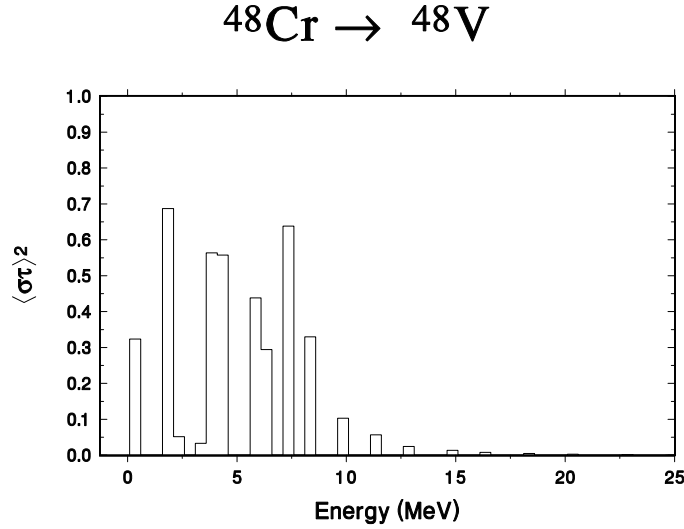


Figure 8: $^{48}\text{Cr} \rightarrow ^{48}\text{V}$ strength function. Full pf shell calculation

Table 8 and fig. 9 collect the information about the Yrast levels. The only complaint we may have with the data is the $B(E2, 8^+ \rightarrow 6^+)$ value but the calculations are telling us much more than they agree with observations.

J	$B(E2, J \rightarrow J-2)$		Q_{spec}	Q_0	
	exp.	th.		from Q_{spec}	from $B(E2)$
2	321 ± 41	228	-29.5	103	107
4	259 ± 83	312	-39.2	108	105
6	>161	311	-39.7	99	100
8	67 ± 23	285	-38.9	93	93
10	>35	201	-22.5	52	77
12		146	-5.3	12	

Table 8: Electromagnetic properties of the Yrast band of ^{48}Cr , $B(E2)$ in $\text{e}^2 \text{fm}^4$, Q in e fm^2

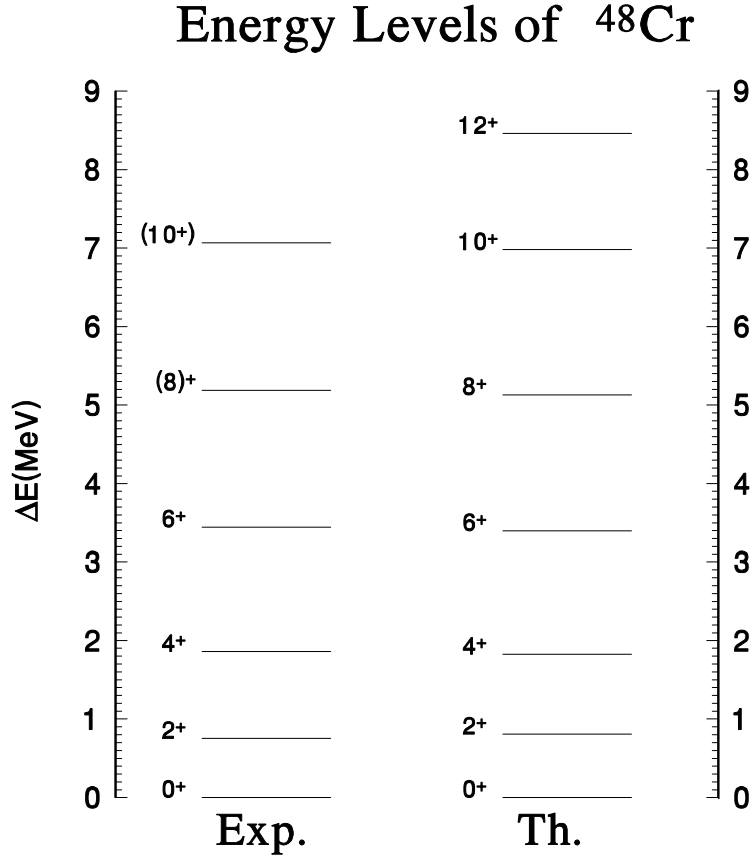


Figure 9: Predicted and experimental Yrast band of ^{48}Cr

According to the criteria of constancy for Q_0 and $J(J+1)$ spacings defined in section 5 we cannot speak of a *good* rotor yet, but we are coming close to it. The $J(J+1)$ behaviour is at best incipient but the constancy of Q_0 is quite convincing.

Two questions come naturally: what is the mechanism?, can we get better rotors?

Table 5 suggests that it is the mixing of $f_{7/2}$ and $p_{3/2}$ orbits that is at the origin of a well defined prolate intrinsic state. If we follow this hint for any $\Delta j = 2$ sequences, it is easy to produce good rotors. The evidence is presented in table 9. It contains more information than necessary to make the point and should be viewed as introductory material for a future communication. Here we limit ourselves to a few comments.

We use the bare KLS force [34] (all realistic interactions are very similar [4, 5, 35, 36] and for this one we have a code [37]). The oscillator frequency is $\hbar\omega = 9$, the spacings between levels are of 1 MeV (higher j orbits coming below) and $Q_0(J)$ is defined in eq. (14).

Under these conditions we obtain truly good rotors. Their stability has been tested under three types of variation.

- i) To affect all $T = 1$ matrix elements by a dilation factor $\lambda \approx 1.5$ mocks surprisingly well

core polarization effects in a major shell [35, 36]. Rotational behaviour persists and may be even emphasized.

- ii) For splittings between levels of 2 MeV the rotational features are eroded but $E_4/E_2 > 3$ in all cases.
- iii) Pairing is the most efficient enemy of good rotors. To go from KLS (bare) to KB (renormalized), $\lambda = 1.5$ (from i)) is sufficient, except for W_{fff}^{01} which should be doubled. Then $E_4/E_2 \approx 2.5$, not far from what is seen in fig. 9.

	$(f_7p_3)^8 \ T = 0$			$(f_7p_3)^4(g_9d_5s_1)^4$		$(g_9d_5s_1)^8 \ T = 0$		$(g_9d_5s_1)^4(h_{11}f_7p_3)^4$		rigid rotor	
J	E	Q_0	E	Q_0	E	Q_0	E	Q_0			
2	0.112	133	0.043	140	0.031	189	0.011	193			
4	0.365	133	0.148	140	0.101	189	0.034	192			
6	0.756	132	0.317	139	0.217	189	0.075	191			
8	1.295	127	0.561	137	0.385	188	0.142	189			
	$\frac{E(J)}{E(2^+)}$	$\frac{Q_0(J)}{Q_0(2^+)}$	$\frac{E(J)}{E(2^+)}$	$\frac{Q_0(J)}{Q_0(2^+)}$	$\frac{E(J)}{E(2^+)}$	$\frac{Q_0(J)}{Q_0(2^+)}$	$\frac{E(J)}{E(2^+)}$	$\frac{Q_0(J)}{Q_0(2^+)}$	$\frac{E(J)}{E(2^+)}$	$\frac{Q_0(J)}{Q_0(2^+)}$	
4	3.26	1	3.32	1	3.44	1	3.29	0.995	3.33	1	
6	6.75	0.992	7.13	1	7.37	0.993	6.74	0.990	7	1	
8	11.56	0.955	12.66	0.995	13.04	0.979	12.72	0.979	12	1	

Table 9: Excitation energies E (in MeV) and intrinsic quadrupole moments Q_0 (in fm²) for the Yrast states of several $\Delta j = 2$ configurations. The notation for the orbits is l_{2j} .

The relevance of these results to real rotors comes directly from Nilsson diagrams which tell us that the onset of deformation at $N \approx 60, 90$ and 136 corresponds to the sudden promotion of two pairs of neutrons (ν) and two pairs of protons (π) to $K = 1/2, 3/2$ orbits originating in the spherical ones $\nu h_{11/2}/\pi g_{9/2}$ $\nu i_{13/2}/\pi h_{11/2}$ and $\nu j_{15/2}/\pi i_{13/2}$ respectively. Naturally we identify the intrinsic state of the eight particles with the one coming out of the diagonalizations, which are possible right now for the first of the three regions, i.e. for the space $(h_{11}f_7p_3)_\nu^4 (g_9d_5s_1)_\pi^4$ (m-scheme dimension $2 \cdot 10^6$). In table 9 we also show the results for $(g_9d_5s_1)_\nu^4 (f_7p_3)_\pi^4$, which we expect to become active for $Z \geq 20, N \approx 40$. The $(g_9d_5s_1)^8$ group is very likely responsible for rotational behaviour in the $A = 80$ region and may be even a candidate for “superbands” at lower masses.

8 ^{48}Mn Truncations and GT strength

Spectroscopically, ^{48}Mn is identical to ^{48}V (to within Coulomb effects). Its decay to ^{48}Cr covers a non negligible fraction of the strength function [38, 39]. Since this process, and similar ones in the region, have been analyzed so far with $t = 1$ calculations, we are going to compare them with $t = 3$ and exact ones. A digression may be of use.

In a decay, the parent is basically an f^n state. Some daughters are also of f^n type but most are $f^{n-1}r$. In a $t = 1$ calculation, both configurations are present but f^n is allowed to mix with $f^{n-1}r$ through W_{ffr} matrix elements while $f^{n-1}r$ is not allowed to go to $f^{n-2}r^2$. At the $t = 2$ level, pairing (i.e. W_{ffrr} matrix elements) comes in and pushes f^n down through mixing with $f^{n-2}r^2$, while $f^{n-1}r$ cannot benefit from a similar push from $f^{n-3}r^3$. It is only at the $t = 3$ level that both f^n and $f^{n-1}r$ states can be treated on equal footing. Now that $t = 3$ calculations are possible up to $A = 58$, it is useful to check their validity.

The results for the half life of ^{48}Mn are collected in table 10. We see that the $t = 3$ truncation is quite acceptable. For the total half-life the $t = 1$ number is not too bad if we remember that full calculations are not always as accurate as they are here. However this relatively good performance owes much to a strong Fermi branch: the partial GT value for $t = 1$ is simply bad. The last line of table 10 gives an idea of the consequences of using calculated instead of observed energies for the transitions.

half-life	$t = 1$	$t = 3$	full	exp
Total	99 ms	133 ms	142 ms	158(22) ms
Partial Fermi	244 ms	244 ms	244 ms	275(20) ms
Partial GT	107 ms	292 ms	340 ms	372(20) ms
Total (theoretical energies)	41 ms	80 ms	116 ms	

Table 10: ^{48}Mn half-lives with different truncations compared with the experimental results

Next we move to the strength functions in figures 10, 11 and 12, where the data show as dots. Globally the three calculations agree in that there is a resonance at $\sim 13\text{ MeV}$ and structure at $\sim 5\text{ MeV}$. Beyond that, $t = 3$ provides a fairly accurate view of the exact shape while $t = 1$ does not. To give an idea of the energetics: the $4^+ T = 1$ analog (IAS) of the ^{48}Mn ground state is at 5.79 MeV in ^{48}Cr , $t = 1$ puts it at 3.64 MeV , $t = 3$ at 4.77 MeV and the exact value is 5.38 MeV (not very good by our standards, see later in section 11).

Now we come to the data and concentrate on the exact calculation. Figure 13 contain very much the same information as figure 12 but instead of $\langle\sigma\tau\rangle^2$ we represent $B(GT)$, affected by the $(0.77)^2$ quenching factor for the calculated numbers. Furthermore, between 6 and 8.5 MeV we have eliminated among these the peaks that fall below the observation threshold (shown as a dashed curve) [39].

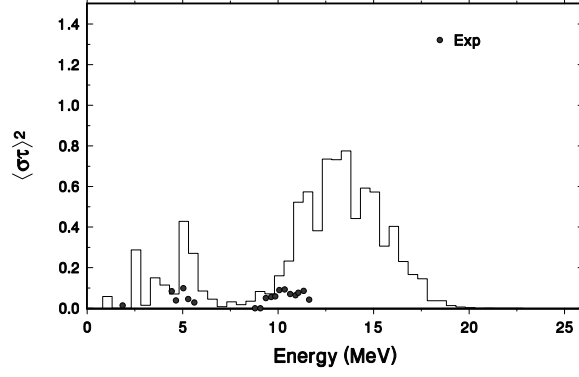
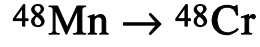


Figure 10: $^{48}\text{Mn} \rightarrow ^{48}\text{Cr}$ strength function. $t = 1$ calculation

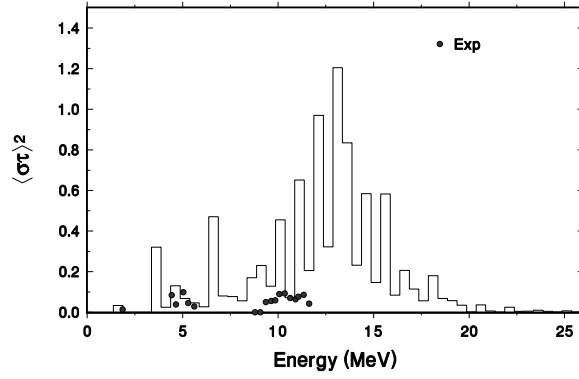
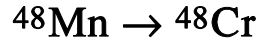


Figure 11: $^{48}\text{Mn} \rightarrow ^{48}\text{Cr}$ strength function. $t = 3$ calculation

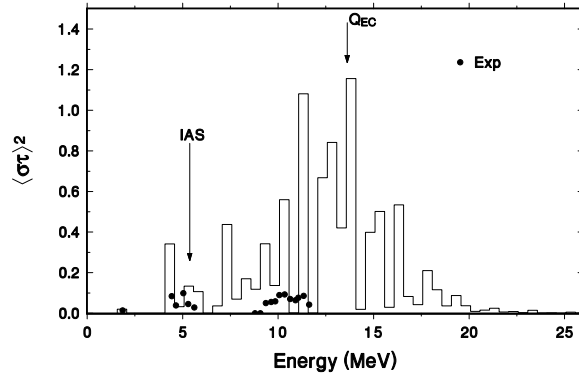
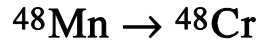


Figure 12: $^{48}\text{Mn} \rightarrow ^{48}\text{Cr}$ strength function. Full calculation

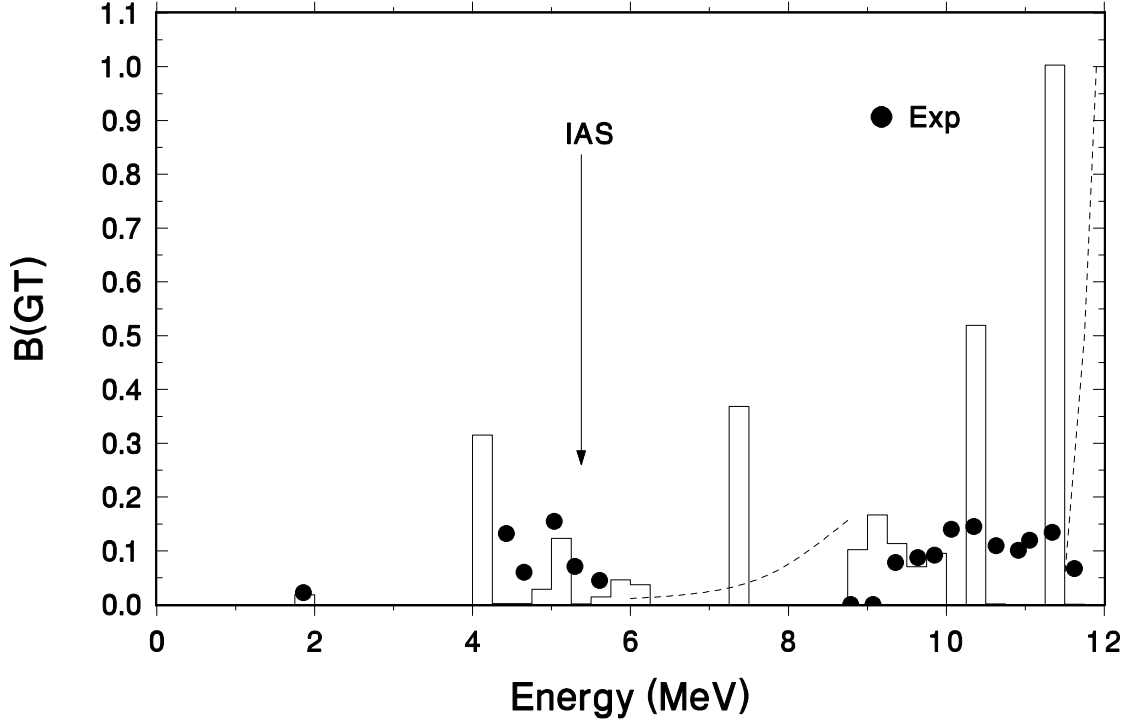
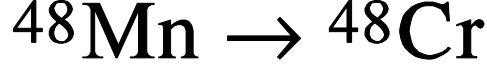


Figure 13: Blow up of the low energy part of figure 12. Here we plot $B(GT)$. Theoretical $B(GT)$ values include standard $(0.77)^2$ quenching. Dotted lines show the observational thresholds [39]. Bins of 250 keV for the calculations (vs. 500 keV in figs. 10-11).

At low energy, the peak at 2 MeV and the cluster of states centered at 5 MeV are very well positioned in the calculations that yield a strength of 0.504 in the interval $[0, 5.75]$ MeV against an observed 0.485. Between 0.75 and 8.75 MeV nothing is seen experimentally, and the only calculated strength above the sensitivity limit is located in two peaks in the $[7.25, 7.50]$ MeV bin. At these energies the calculated levels are not yet eigenstates of the system but doorways whose strength (0.405) will be fragmented (see next section).

Above 8.75 MeV observation resumes through delayed protons yielding $B(GT) = 1.073$ in the $[8.75, 11.75]$ MeV interval versus the calculated 2.07 mostly found in two bins at $[10.25, 10.50]$ and $[11.25, 11.50]$ MeV. At these energies the density of levels is high and fragmentation will become important. Furthermore, half of the calculated strength is in the last bin, dangerously close to the abrupt rise in the sensitivity threshold. Therefore, before we conclude that experiments demand *anomalous* quenching (i.e.: beyond the standard value) we shall analyse more closely what is being calculated and what is being measured.

9 Quenching, shifting and diluting GT strength

From all we have said about GT transitions, a broad trend emerges: low lying levels are *very well* positioned and within minor discrepancies have the observed GT strength once standard quenching is applied. The examples of good energetics are particularly significant for the group around 5 MeV in ^{48}Cr and the 1^+ levels in ^{48}Ti (fig. 3) and ^{48}Sc (table 2), that have experimental counterparts within 100 keV more often than not. The discrepancies are related to the shortish half-life of ^{48}Sc and ^{48}V , a slight lack of spin strength in the lowest states of ^{48}Ti (ref. [17]) and —perhaps— with the tail of the resonant structure in ^{48}Cr discussed in the preceding section.

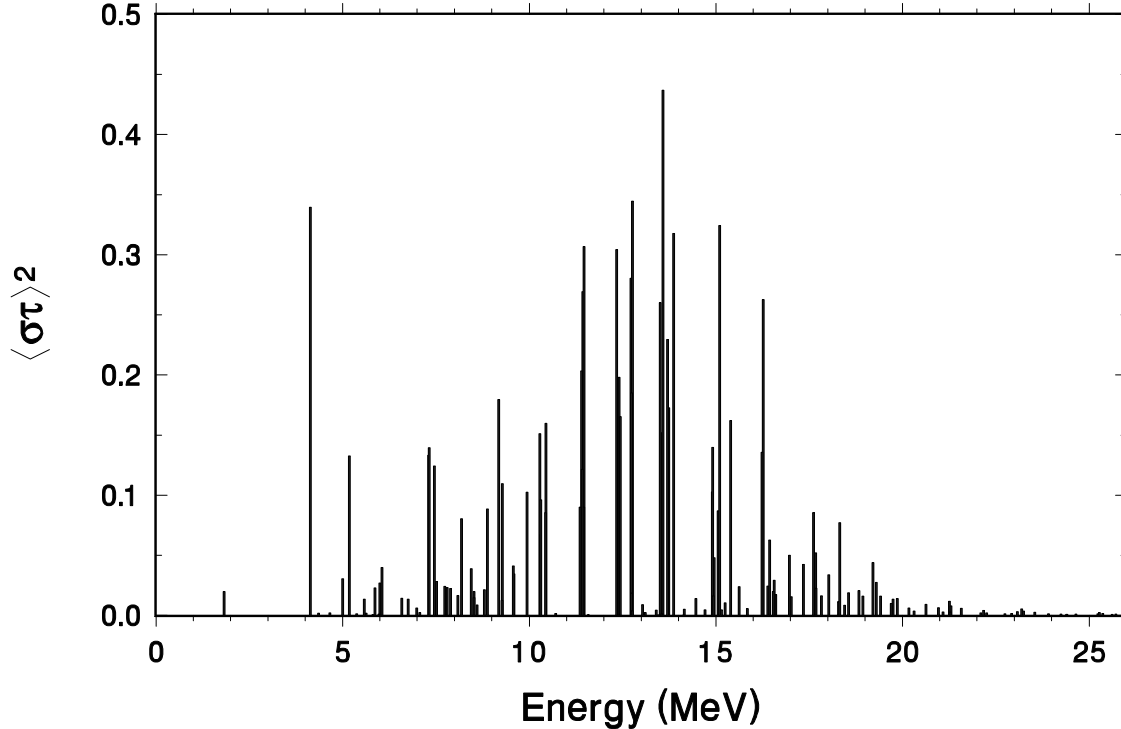
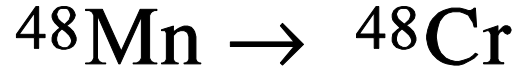


Figure 14: Same as figure 12 but without any binning

To cure the discrepancies we need a mechanism that may affect very slightly the overall GT distribution, without affecting the positions and other properties of the underlying levels, which are very well reproduced. Here, it is useful to remind how the strength function is obtained.

First, we define a state $|s\rangle$ by acting on the parent, $|s\rangle = \sigma\tau|i\rangle S^{-1/2}$ which exhausts by construction the sum rule $S = \langle i|(\sigma\tau)^2|i\rangle$, and then evaluate the amplitude of $|s\rangle$ in each daughter state by doing Lanczos interactions using $|s\rangle$ as pivot [17]. The first iteration produces the centroid and variance of the strength function, $E_s = \langle s|H|s\rangle$ and $v_s = \langle s|H^2 - E_s^2|s\rangle$

respectively. As the number of iterations ν increases, the strength —originally concentrated at E_s — is fragmented into ν peaks. The lowest converge to exact eigenstates (with their exact share of the total sum rule) at the rate of roughly one every 6-10 iterations. Figure 14 is the high resolution version of fig. 12 and shows the situation after 60 iterations for each of the JT values ($J = 3, 4, 5$; $T = 0, 1, 2$). It is only below approximately 6 MeV that we have a complete picture of the spectrum. Above, many thousand states are waiting to come and erode the strong peaks.

Let us examine first the global properties associated with S and E_s and then turn to the consequences of local fragmentation.

Quenching. Calculations always produce too much strength, that has to be reduced by a quenching factor, which is the stronger (i.e. smaller) the most drastic the truncation [17]. For exact calculations in *one major shell* ($0\hbar\omega$), S has to be reduced by $(0.77)^2$, *which is very much the value demanded by the “violation” of the model independent sum rule* (16). There is very little we can do *within a $0\hbar\omega$ calculation* to change this state of affairs.

Shifting. Contrary to S , which depends on geometry (16) and on overall properties of H , E_s may be significantly affected by small changes in the $\sigma \cdot \sigma$ and $\sigma\tau \cdot \sigma\tau$ contributions to H . In ref. [36] it is shown that these spin-spin terms are very strong, especially the second, and may differ from force to force by some 20% (the corresponding constants e_{1+0} and e_{1+1} in ref. [36] are related, but not trivially, to the Migdal parameters g and g'). Therefore, the mechanism to cure the small discrepancies we have mentioned may well come from modifications in these numbers, that would produce small overall *shifts* of the distribution, and nothing else.

Now we return to the quenching problem. In view of discrepancies between (p, n) and β^+ data for ^{37}Ca , the extraction of S from the former has been recently criticized [40, 41]. The problem was compounded by the fact that calculations with Wildenthal’s W interaction suggested that standard quenching did not seem necessary. This illusion was dispelled by Brown’s analysis [42], showing that the interaction was at fault. It is very interesting to note that what is called 12.5p in [42] is none other than KB, while CW—which gives the best results—is very basically a minimally modified KB that can be safely assimilated to KB1 or KB3.

Diluting. Brown’s analysis contains another important hint: once normalized by the $(0.77)^2$ factor, the CW calculations follow smoothly the data within the β window, but then produce too much strength when compared with the (p, n) reaction. The suggestion from fig. 14 is that in regions where the density of levels becomes high, fragmentation may become so strong that much strength will be so *diluted* as to be rendered unobservable. The difference between the $A = 37$ and $A = 48$ spectra is that in the former the effect is almost exclusively due to intruders, while in the latter the density of pf states is high enough

to produce substantial dilution by itself. Which brings us back to the problem of the amount of strength calculated between 8.75 and 11.75 MeV in ^{48}Cr , double the measured value. Some shifting may be warranted to reduce the discrepancy, but fig. 14 suggest very strongly that dilution be made responsible for it (i.e. for anomalous quenching)

From all this, it follows that simultaneous measurements of β^+ and (p, n) strength are very much welcome in pairs of conjugate nuclei where the β^+ release energy is large, the $0\hbar\omega$ spectrum is dense and high quality calculations are feasible. We propose the following candidates:

β^+	(p, n)
$^{45}\text{Cr} \rightarrow ^{45}\text{V}$	$^{45}\text{Sc} \rightarrow ^{45}\text{Ti}$
$^{46}\text{Cr} \rightarrow ^{46}\text{V}$	$^{46}\text{Ti} \rightarrow ^{46}\text{V}$
$^{47}\text{Mn} \rightarrow ^{47}\text{Cr}$	$^{47}\text{Ti} \rightarrow ^{47}\text{V}$
$^{48}\text{Fe} \rightarrow ^{48}\text{Mn}$	$^{48}\text{Ti} \rightarrow ^{48}\text{V}$.

To conclude: a theoretical understanding of standard quenching demands that we look at the full wavefunction and not only at its $0\hbar\omega$ components. Experimentally, what has to be explained is the disappearance of strength, i.e. standard *and* anomalous quenching (as observed in ^{48}Cr). Dilution will no doubt play a role in both, but the latter may be observed already by comparisons with $0\hbar\omega$ calculations.

10 The validity of *monopole* modified realistic interactions

To answer with some care the question raised in the introduction we review briefly the work related to monopole corrections.

The first attempt to transpose the results of refs. [4, 5] to the *sd* shell met with the problem that the interaction had to evolve from ^{16}O to ^{40}Ca . A linear evolution was assumed, but it was shown that the centroids followed more complicated laws demanding an excessive number of parameters [43].

The solution came in ref. [35], by adopting a hierarchy of centroids and noting that the realistic matrix elements depend on the harmonic oscillator frequency very much as

$$W_{rstu}^{JT}(\omega) = \frac{\omega}{\omega_0} W_{rstu}^{JT}(\omega_0), \quad (17)$$

thus displacing the problem of evolution of H to one of evolution of ω . The classical estimate $\hbar\omega = 40A^{-1/3}$ [44] relies on filling oscillator orbits and on adopting the $r = r_0A^{1/3}$ law for radii, which nuclei in the *p* and *sd* shells do not follow. Therefore it was decided to treat ω as a free parameter for each mass number and then check that the corresponding oscillator orbits reproduce the observed radii. This turned out to work very well and to produce very good spectroscopy in all regions where exact calculations could be done.

The method relies on the rigorous decomposition of the full Hamiltonian as $\mathcal{H} = \mathcal{H}_m + \mathcal{H}_M$, where the monopole part \mathcal{H}_m is responsible for saturation properties, while \mathcal{H}_M contains all the other multipoles. Upon reduction to a model H , \mathcal{H}_m is represented by H_m , which contains the binding energies of the closed shells, the single particle energies and the centroids. Everything else goes to H_M , which nevertheless depends on \mathcal{H}_m through the orbits, in principle selfconsistently extracted from \mathcal{H}_m [35, 36, 45]. The program of minimal modifications now amounts to discard from the nucleon-nucleon potential the \mathcal{H}_m part and accept all the rest, unless some irrefutable arguments show up for modifying something else. On the contrary \mathcal{H}_m is assumed to be purely phenomenological and the information necessary to construct it comes mostly from masses and single particle energies [45].

The proof of the validity of the realistic \mathcal{H}_M through shell model calculations depends on the quality of the monopole corrections. In regions of agitated radial behaviour we have to go beyond the oscillator approximation. In particular, the sd shell radii can be reproduced practically within error bars by Hartree-Fock calculations with Skyrme forces with orbital fillings extracted from the shell model wave functions [46]. Obviously the $d_{5/2}, s_{1/2}$ and $d_{3/2}$ orbits are poorly reproduced by a single ω , and obviously this makes a difference in the two body matrix elements [34] (work is under progress on this problem).

Therefore, in the sd shell—to match or better the energy agreements obtained with Wildenthal’s famous W (or USD) interaction [47, 48]—we have to push a bit further the work of ref. [35].

When we move to the pf shell, no such efforts are, or were, necessary. Because of $f_{7/2}$ dominance, it is much easier to determine the centroids: the V_{rr}^T values are no issue, the crucial V_{ff}^T ones can be read (almost) directly from single particle properties on ^{49}Ca and ^{57}Ni , and we are left with V_{ff}^T ; only two numbers. Once we have good enough approximations for the centroids we can do shell model calculations to see how the rest of H (i.e. H_M) behaves. In ref. [23] it was found that H_M behaves quite well, but much better in the second half of the f^n region: $A = 48$ happens to be the border beyond which quite well becomes very well. Hence the remark in the second paragraph of the introduction.

The trouble at the beginning of the region was attributed at the time to intruders, but now we know that radial behaviour must be granted its share. It is here that KB3 comes in. Although eq. 5 has only cosmetic effects, its origin is not cosmetic: it was meant to simulate necessary corrective action *not related to the presence of intruders*. It reflects the fact that in the neighborhood of ^{40}Ca the interaction works better if the spectrum of ^{42}Sc is better reproduced, while at $A = 48$ and after, the KB interaction—not very good in ^{42}Sc —needs no help, except in the centroids, as we have shown.

Most probably this says something about radial behaviour at the beginning of the region. It is poorly known except in the Ca isotopes, where it is highly non trivial [49]. The indications are that when shell model calculations demand individual variations of matrix elements in going from nucleus to nucleus the most likely culprits are the single particle orbits. And the

indications are that at $A = 48$ the need for such considerations disappears.

All this is to say that $A = 48$ happens to be a good place for a test of the interaction and KB1 passes it with honours. It also amounts to say that it is not an accident but part of the general statement that monopole corrected realistic interactions are the ones that *should* be used in calculations.

It is important to stress that monopole corrections are both necessary and sufficient.

Doing less amounts to run great risks as illustrated by the $T = 2$ states in $A = 56$. Using KB leads to a very good looking spectrum in a $t = 2$ calculation of ^{56}Fe [50], but ignores the fact that the force would produce nonsense for $T = 0$. (For $T = 2$, KB1 or KB3 gives results that are even better looking than those of KB, and somewhat different).

Doing more, under the form of extended fits of all matrix elements, has become unnecessary and may be misleading as illustrated by the problems encountered by W, the most famous of the fitted interactions (section 9, [42]). Still, a full explanation of its success in terms of monopole behaviour remains a challenge.

11 Note on binding energies

Our interaction overbinds all the $A = 48$ nuclei by about the same amount, indicating the need of small corrections in the centroids. The addition of an overall $Vn(n-1)/2$ term with $V = 28$ keV, leads to the binding energies in table 11, which have been Coulomb corrected by subtracting ($n = \pi + \nu$, $\pi =$ protons, $\nu =$ neutrons) [4]

$$\begin{aligned} H_{\text{coul}} &= V_{\pi\pi}\pi(\pi-1)/2 + V_{\pi\nu}\pi\nu + 7.279\pi \text{ MeV} \\ V_{\pi\pi} &= 0.300(50) \text{ MeV}, V_{\pi\nu} = -0.065(15) \text{ MeV}. \end{aligned} \tag{18}$$

	Ca	Sc	Ti	V	Cr	Mn	Fe
Exp	7.04	13.35	23.82	26.70	32.38	26.86	
Th	7.10	13.35	23.79	26.80	32.17	26.80	23.79

Table 11: Nuclear two-body energies (MeV), $A = 48$

For ^{48}Fe we obtain $BE = 385.37 \text{ MeV}$, leading to a decay energy of 10.94 MeV for $^{48}\text{Fe} \rightarrow ^{48}\text{Mn}$. The most recent estimate of Wapstra, Audi and Hoekstra [51] gives $BE(^{48}\text{Fe})=385.21 \text{ MeV}$. The precision of subtractions [16] can be checked through the position of the analog of ^{48}V in ^{48}Cr , experimentally at 5.79 MeV against the Coulomb corrected value of 5.68 MeV in table 11. As noted in section 8, for this state there is a 400 keV discrepancy between experiment and calculation, high by our standards. It probably indicates

the need of some more sophistication in the readjustment of monopole terms than the 28 keV we have suggested. Note that the theory-experiment differences in table 11 are typical of the results throughout the paper.

12 Conclusions

Since much of the sections 9 and 10 was devoted to drawing conclusions about the two main problems addressed, we shall only sum them up:

- i) The detailed agreement with the data lends strong support to the claim that minimally monopole modified realistic forces are the natural and correct choice in structure calculations.
- ii) The description of Gamow-Teller strength is quite consistent with the data, to within the standard quenching factor. The calculations strongly suggest that dilution due to fragmentation makes much of the strength unobservable.

Two by-products emerge from the calculations. The first is mainly technical:

- iii) Truncations at the $t = 3$ level are reasonable in the lower part of the pf shell. In general, however, truncations are a dangerous tool and it would be preferable to replace them by some other approximation method.

The second by-product is more interesting:

- iv) The calculations provide a very clean microscopic view of the notion of intrinsic states and of the conditions under which rotational motion sets in.

Acknowledgements

This work has been supported in part by the DGICYT (Spain) grant PB89-164 and by the IN2P3 (France)-CICYT (Spain) agreements.

References

- [1] J.N. Ginocchio and J.B. French, Phys. Lett. **7** (1963) 137.
J.N. Ginocchio, Phys. Rev. **144** (1966) 952.
- [2] J.D. Mc Cullen, B.F. Bayman and L.Zamick, Phys. Rev. **B4** (1964) 515.
- [3] H. Horie and K. Ogawa, Nucl. Phys. **A216** (1973) 407.
- [4] E. Pasquini, Ph. D. Thesis CRN/PT 76-14, Strasburg 1976.

- [5] E. Pasquini and A.P. Zuker, “Physics of Medium Light Nuclei”, Florence 1977, P. Blasi and R. Ricci eds. (Editrice compositrice, Bologna 1978).
- [6] A.G.M. van Hess and P.W.M. Glaudemans, Z. Phys. **A303** (1981) 267.
- [7] R.B.M. Mooy and P.W.M. Glaudemans, Z. Phys. **A312** (1983) 59.
- [8] R.B.M. Mooy and P.W.M. Glaudemans, Nucl. Phys. **A438** (1985) 461.
- [9] K. Muto and H. Horie, Phys. Lett. **B138** (1984) 9.
- [10] A. Yokohama and H. Horie, Phys. Rev. **C31** (1985) 1012.
- [11] K. Muto, Nucl. Phys. **A451** (1986) 481.
- [12] J.B. Mc Grory, B.H. Wildenthal and E.C. Halbert, Phys. Rev. **C2** (1970) 186.
- [13] J.B. Mc Grory and B.H. Wildenthal, Phys. Lett. **B103** (1981) 173.
- [14] J.B. Mc Grory, Phys. Rev. **C8** (1973) 693.
- [15] B.J. Cole, J. Phys. **G11** (1985) 481.
- [16] W.A. Richter, M.G. Van der Merwe, R.E. Julies and B.A. Brown, Nucl. Phys. **A523** (1991) 325.
- [17] E. Caurier, A. Poves and A.P. Zuker, Phys. Lett. **B256** (1991) 301.
- [18] K. Ogawa and H. Horie, “Nuclear weak processes an nuclear structure”, M. Morita et al. eds. (World Scientific, Singapore 1990).
- [19] E. Caurier, A. Poves and A.P. Zuker, Phys. Lett. **B252** (1990) 13.
- [20] J. Engel, W.C. Haxton and P. Vogel, Phys. Rev. **C46** (1992) 2153.
- [21] W. Kutschera, B.A. Brown and K. Ogawa, Riv. Nuovo Cimento Vol. **1** n° 12 (1978).
- [22] A. Poves, E. Pasquini and A.P. Zuker, Phys. Lett. **B82** (1979) 319.
- [23] A. Poves and A.P. Zuker, Phys. Rep. **70** (1981) 235.
- [24] T.W. Burrows, Nuclear Data Sheets **68** (1993) 1.
- [25] E. Caurier, Code ANTOINE (Strasbourg, 1989).
- [26] E. Caurier, A. Poves and A.P. Zuker, Proc. of the Workshop “Nuclear Structure of Light Nuclei far from Stability. Experiment and Theory.” Obernai. G. Klotz ed. (CRN, Strasbourg, 1989).

- [27] R.R. Whitehead in “Moment methods in many fermion systems” B.J. Dalton et al. eds. (Plenum, New York, 1980).
- [28] T.T.S. Kuo and G.E. Brown, Nucl. Phys. **A114** (1968) 241.
- [29] A.R. Edmonds, “Angular Momentum in Quantum Mechanics” (Princeton, N.J. 1960).
- [30] D.H. Wilkinson and B.E.F. Macefield, Nucl. Phys. **A232** (1974) 58.
- [31] W. Bambynek, H. Behrens, M.H. Chen, B. Graseman, M.L. Fitzpatrick, K.W.D. Ledingham, H. Genz, M. Mutterer and R.L. Intemann Rev. Mod. Phys. **49** (1977) 77.
- [32] D.G. Fleming, O. Nathan, H.B. Jensen and O. Hansen, Phys. Rev. **C5** (1972) 1365.
- [33] P. Raghavan, Atomic Data and Nuclear Data Tables **42** (1989) 189.
- [34] S. Kahana, H.C. Lee and C.K. Scott, Phys. Rev. **180** (1969) 956.
- [35] A. Abzouzi, E. Caurier and A.P. Zuker, Phys. Rev. Lett. **66** (1991) 1134.
- [36] M. Dufour and A.P. Zuker, preprint CRN 93-29, proposed to Physics Reports, (1993).
- [37] H.C. Lee. *private communication*, (1969).
- [38] T. Sekine, J. Cerny, R. Kirchner, O. Klepper, V.T. Koslowsky, A. Plochocki, E. Roeckl, D. Schardt, B. Shenill and B.A. Brown, Nucl. Phys. **A467** (1987) 93.
- [39] J. Szerypo, D. Bazin, B.A. Brown, D. Guillemaud-Muller, H. Keller, R. Kirchner, O. Klepper, D. Morrissey, E. Roeckl, D. Schardt, B. Sherrill, Nucl. Phys. **A528** (1991) 203.
- [40] E.G. Adelberger, A. Garcia, P.V. Magnus and D.P. Wells, Phys. Rev. Lett. **67** (1991) 3658.
- [41] M.B. Aufderheide, S.D. Bloom, D.A. Resler and D.C. Goodman, Phys. Rev. **C46** (1992) 2251.
- [42] B.A. Brown, Phys. Rev. Lett. **69** (1992) 1034.
- [43] A. Cortés and A.P. Zuker, Phys. Lett. **B84** (1979) 25.
- [44] A. Bohr and B. Mottelson, “Nuclear Structure” (Benjamin, NY 1969).
- [45] A.P. Zuker, preprint CRN 92-16, to be published in Nucl. Phys.
- [46] A. Abzouzi, J.M. Gomez, C. Prieto and A.P. Zuker, CRN Strasbourg Annual Report (1990) p.15.
- [47] B.H. Wildenthal, Prog. Part. Nucl. Phys. **11** (1984) 5.
- [48] B.A. Brown and B.H. Wildenthal, Annual Rev. Nucl. and Part. Sci. **38** (1988) 292.

- [49] E. Caurier, A. Poves and A.P. Zuker, Phys. Lett. **B96** (1980) 15.
- [50] H. Nakada, T. Otsuka and T. Sebe, Phys. Rev. Lett. **67** (1991) 1086.
- [51] A.H. Wapstra, G. Audi and R. Hoekstra, Atomic Data and Nuclear Data Tables **39** (1988) 281.